Ignition and Flashover of Reduced Scale Compartments with Timber Ceilings

Ignition and Flashover of Reduced Scale Compartments with Timber Ceilings

James Greer[a*], Sergio Caponi[a], Rory M. Hadden[a], Angus Law[a]

[a]School of Engineering, The University of Edinburgh, Scotland, J.Greer@ed.ac.uk

*Corresponding author

Highlights:

- Timber
- Ceiling ignition
- Flashover

Abstract:

Experiments on reduced-scale compartments with timber ceilings and floors were conducted to investigate the ignition of the ceiling and growth to flashover. Pool fires of various sizes were ignited and measurements were made of temperature in the plume and ceiling jet, and mass of the timber ceiling and floor. The compartment geometry was also systematically varied. The results showed that ignition of the ceiling occurred when the measured temperature at ceiling level was between 328°C and 347°C. This aligned with intermittent flame impingement on the ceiling from the initiating fire. Following ignition of the ceiling, in most cases the fire subsequently spread across the ceiling resulting, ultimately, in ignition of the floor. It was found that duration of preheating of the ceiling (by the ceiling jet) strongly influenced flame spread. In some cases, ignition occurred, but did not result in continuous flame spread across the ceiling – in these cases it was found that the ceiling jet was cooler due to wider geometry of the compartment. The data were compared against existing correlations from the literature, and it was found that existing methods may be used to predict whether ignition of the ceiling may occur and the conditions for flashover.

Keywords: Timber; Compartment Fires; Ignition; Fire Growth; Heat Transfer

Nomenclature

$\boldsymbol{A}$	Area of pool fire (cm^2)
$\boldsymbol{d}$	Depth of the compartment (mm)
$\boldsymbol{h}$	Height of the compartment (mm)
$\dot{\boldsymbol{m}}$	Burning rate of the fuel prior to the ignition of the ceiling (g/s)
$\dot{\boldsymbol{Q}}$	Heat release rate (HRR) (kW)
$\dot{\boldsymbol{Q}}_{\boldsymbol{c}}$	Convective portion of the heat release rate(kW)
$\boldsymbol{r}$	Distance along the ceiling from point of flame impingement (mm)
$\boldsymbol{t}_{\boldsymbol{ig,c}}$	Ignition time of the ceiling (s)
$\boldsymbol{t}_{\boldsymbol{ig,f}}$	Ignition time of the floor (s)

Δt	Time difference between ignition of the ceiling and when flames emerged across the entire width of the ceiling (s)
Δt_{ig}	Time difference between ignition of the ceiling and the floor (s)
T	Temperature of the gas beneath the ceiling, above the centre of the pool fire, prior to ignition of the ceiling (°C)
T_{ff}	Temperature of the gas beneath the ceiling, in the far field (°C)
ΔT	Rise in temperature (°C)
w	Width of the compartment (mm)
x	Horizontal distance from point of impingement (mm)
z	Distance between the ceiling and the base of the fire (mm)
η	Plume temperature correlation coefficient (-)

1. Introduction

The ignition of combustible ceilings, and subsequent fire growth is of increasing relevance to fire safety in the built environment due to the increasing use of engineered timber in buildings [1]. Timber is a combustible material, and it has been shown that when used as a lining product within a compartment, the contribution of the timber has the potential to accelerate fire growth [2]. Many jurisdictions therefore place limits on the use of timber lining materials for some applications. Characterising the hazard posed by combustible ceilings is therefore essential when designing compartments with exposed timber ceilings.

Timber is a material about which there is a wealth of literature [3,4]. Although there are relatively few studies which specifically explore ignition and fire spread in the ceiling configuration, the concepts of ignition theory and the controlling mechanisms are likely to still apply. The material properties which govern ignition and fire growth are well established [5,6]. While the critical heat flux is a system parameter, and values obtained from previous work are unlikely to translate directly to the ceiling configuration, the role of thermal inertia and a temperature which characterises the onset of pyrolysis are still likely to be applicable despite the change in orientation.

Ignition of the ceiling is typically driven by heat transfer from the buoyant plume from a fire arising from the moveable fuel load. When the rising buoyant plume impinges on the ceiling it will transition from rising vertically to flowing radially outwards from the point of impingement. As the hot gases spread across the ceiling, they will entrain ambient air, causing the temperature of the gases beneath the ceiling to decrease with distance from the point of impingement. Therefore, the maximum temperature of the gas beneath the ceiling and hence the location where the ceiling will pyrolyse first, will occur at the point of impingement. Buoyant plumes from fires are a well-characterised phenomenon. The classical description by Morten et al. [7], allows the mass entrainment of an axisymmetric plume to be described and the temperature of the gas within the plume to be predicted as a function of height. Behaviour towards the base of the plume (i.e. in

and above the flame) was described by McCaffery based on measurements from diffusions flames. This work distinguished between the continuous, intermittent, and plume region [8]. These principles are now firmly established within the regulatory literature and guidance documents that are used by engineers for the design of various engineering systems [9,10].

Characterising the ignition of timber ceilings by buoyant plumes within compartments is therefore a problem at the intersection of various topics where there is a wealth of established knowledge. The approach explored here seeks to use existing plume theory to define the thermal environment near the timber ceiling and relate this to the parameters which control the ignition of timber. This aim is to determine appropriate indicators for ignition of the timber ceiling and, once the ceiling has ignited, the subsequent fire development.

1.1. Previous work

The ignition of timber has been studied in various configurations for more than a century. Bartlett [4] summarised the extensive literature on the ignition of timber. In standardised conditions, critical heat fluxes for piloted and unpiloted ignition are approximately 10-13 kW/m^2 and 25-33 kW/m^2 respectively [4]. Such data are potentially useful for examining the ignition of timber ceilings. However, it should also be recognised that in the inverted (ceiling) condition, critical heat fluxes and times to ignition may vary compared to samples tested in the horizontal (floor) condition. Shields et al. [11], for example, found that times to ignition increased threefold for samples tested in the ceiling configuration compared to the floor configuration. These results demonstrate that values for critical heat fluxes or times to ignition that were obtained in "floor" configurations cannot necessarily be applied to "ceiling" configurations. Nevertheless, surface temperature of timber remains a useful metric as it is indicative of the rate of pyrolyzate production – and the potential for these products to ignite in the presence of a pilot. The rate of timber pyrolysis is found to rapidly increase between 300°C and 500°C which may be a useful criterion for developing this kind of methodology.

The temperature rise within a buoyant plume has been described by McCaffrey [8] as follows:

$$\Delta T \propto \left(\frac{z}{\dot{Q}_C^{2/5}}\right)^{\eta} \qquad \text{Equation 1}$$

Where z is the vertical distance to the base of the fire, $\dot{Q}_c$ is the convective portion of the heat release rate (HRR), and η is a dimensionless coefficient which varied as a function of height. This correlation was developed for buoyant plumes that were rising free from obstructions. When a rising plume impinges on a ceiling it will be deflected radially; this was characterised by Alpert [12]. Conditions in the ceiling jet were scaled with heat release, height of rise, and radial distance from a central free-field fire. It was found that:

$$\Delta T \propto \left(\frac{\dot{Q}_c/r}{z}\right)^{2/3}$$ Equation 2

However, the focus of Alpert's work was on the detection conditions for thermally actuated and smoke actuated detectors rather than a study of ceiling ignition.

You and Faeth [13] also studied the heat transfer to a ceiling from an impinging plume. They found that convection dominated the heat transfer on the ceiling, with radiation comprising less than 20% of the total heat transferred. They also observed that the highest rates of heat transfer (60 kW/m^2) were in the region of the stagnation point. Kokkala [14,15] conducted a series of experiments to study the heat transfer to and ignition of PMMA ceilings. The experiments featured a ~300 mm disc of fuel onto which a plume from a fixed diameter burner impinged. Heat flux was measured at the surface of the solid using a water-cooled heat flux gauge, and gas phase temperature was measured using thermocouples. This work linked the heat transfer on the ceiling to scaling of the plume correlation (Eq. 1) but found higher heat fluxes than You and Faeth. This was attributed to the nature of the experimental setup in which the source was a gas burner with a fixed diameter (64 mm). Thus, for higher heat release rates (achieved by higher fuel flow rates from the same orifice), the burner tended towards a momentum driven jet flame rather than a buoyancy driven diffusion flame.

Kokkala [15] analysed the time to ignition and attempted to correlate this with the inverse square of applied heat flux. However, there was substantial scatter and it was concluded that attempting to fit a line though the data was "unreasonable". In recent years, researchers have expressed a renewed interest in the conditions under which ceiling configurations will ignite. Of particular relevance in relation to this study is work by Nothard et al. [16], and Kotsovinos et al. [17]. Kotsovinos et al. reported the ignition of the ceiling occurred when flames impinged on the soffit. Their data suggests that this occurred when reported gas temperatures were in the region of 300 °C. Nothard et al. linked ignition of the ceiling to the applied heat flux and associated ignition delay time. Again, these data suggest that temperature measurement may provide a useful indicator of potential for ignition – where directly estimating the heat flux or equating this to small scale tests may not be immediately possible.

Once combustible ceiling has ignited, there is the potential for the flames to spread. Flame spread on materials in various orientations has been extensively studied (e.g. [18], [19]). In general, the rate of spread is increasingly governed by convective heat transfer as the orientation of a specimen changes from the vertical to ceiling condition. However, although spread on a ceiling is classified as concurrent flame spread, the phenomenon is less well studied in this configuration. Hinkley and Wraight reported a series of experiments on combustible ceiling linings [20]. These experiments involved a burner placed below a combustible ceiling – with the flames from the burner extending along the ceiling. Burning rate of the ceiling was measured, but rate of fire spread was not directly reported. It was noted that the heat transfer from the hot flames and gases would be sufficient to ignite a combustible floor – and thereafter the fire behaviour would likely be dominated by a shortage of air.

More recently, authors have studied char patterns from impinging burners, but did not explore flame spread [21]. Notwithstanding the relative paucity of information on flame spread in the ceiling orientation, various authors have noted the importance of the presence of ceiling flames in creating the conditions necessary for flashover. Commonly accepted definitions for the onset of flashover are achieving a heat flux of 20 kW/m^2 at low level within the compartment; ceiling temperatures of 600 ºC; and flaming outside the compartment [5]. In the context of compartment with timber linings, the experiments of Nothard et al. [16] are particularly notable. These were based on a "long" compartment configuration – where the fire was allowed to spread on the combustible floor. The authors observed that ignition of the Cross Laminated Timber (CLT) was followed by a transition from a "travelling" or "spreading" fire, to a "fully involved fire", where the flame front progressed rapidly through the compartment.

From this short review it is evident that:

- Ignition of timber in the ceiling configuration is influenced by both the orientation (i.e. being in the "ceiling" condition), and also by the local conditions within the impinging plume.
- The onset of pyrolysis around 300°C may be a useful criterion for the ignition of timber.
- Temperatures on the centreline of a plume from a diffusion flame roughly follows the trends described by Eq. 1, even when the rise of the plume is interrupted by impingement on a ceiling. Thus, while the HRR of the initiating fire is important, height is the parameter with the strongest influence on the temperature of the gas at the location of impingement.
- Flame spread on a ceiling is a concurrent flow condition that is likely to be dominated by convective heat transfer from the gases at the ceiling.
- Once a flame has spread across the ceiling, the heat flux generated by the flames beneath the ceiling is capable of promoting ignition of items at floor level, accelerating the transition to ventilation controlled burning.

These observations allowed the authors to design an experimental study to investigate the applicability of existing work to the ignition and flashover of compartments with timber ceilings.

2. Methodology

As noted previously, the key parameters of interest that feature in previous work are the HRR ($\dot{Q}$) and the height of rise of the plume (z). The HRR of the initiating fire and separation between the ceiling and base of the fire were systematically varied as part of an experimental study.

Pool fires of varying diameters were used to achieve steady fires with different HRRs. The HRR was determined through measurements of the mass and calculation of the mass loss rate (MLR) of the fuel during the experiment. The primary fuel used was paraffin (90%); heptane (10%) was added to the mixture so that the fuel mixture could be easily ignited. Square pans of between 50.4 cm^2 and 154 cm^2 were used (giving HRRs of between around 1.5 kW and 5.2 kW). The fuel was ignited using a small flame.

An experimental apparatus was designed (Figure 1) which could allow the height of the compartment to be adjusted. The front of the compartment was open. The pool fire area (A), depth (d), width (w) and height (h) of the compartment were varied parametrically – with the primary emphasis being on the variation of $\dot{Q}$ and h.

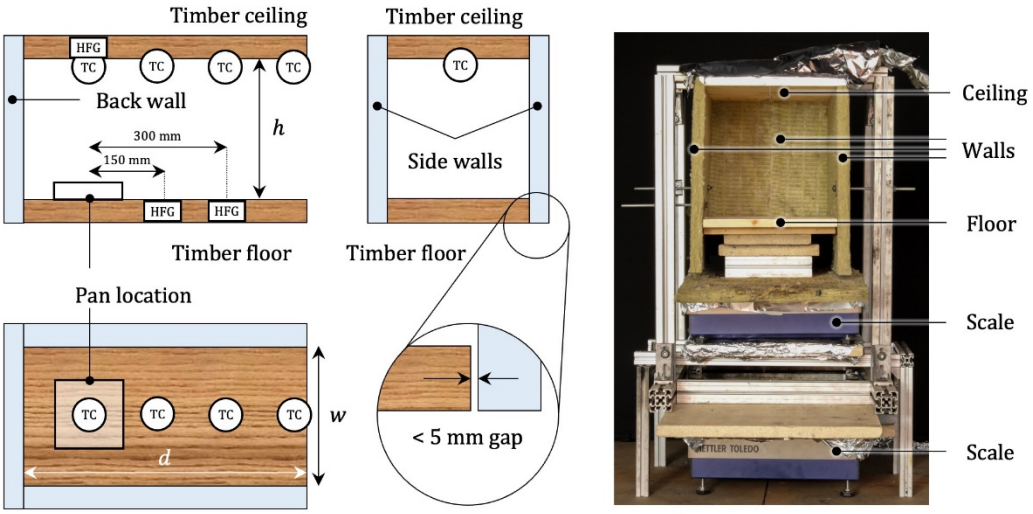

Figure 1 Diagram of the reduced scale compartment presented alongside a labelled photograph of the experimental setup.

A base configuration with a depth of 600 mm, a width of 300 mm and a height of 300 mm was selected. The dimension of 600 mm was selected as this was readily available from commercial suppliers. From this configuration the compartment height was increased to 345 mm and 390 mm. The impact of compartment width was also assessed with a larger configuration; where the depth and width of the compartment were doubled to 1200 mm and 600 mm respectively. For each of these configurations the pool area was varied. This approach allowed a scaling analysis to be conducted in accordance with Eq. 1. A full list of geometries and HRRs for the experiments is presented as part of Table 1, in the results section.

The ceiling and floor of the compartment were 18 mm thick untreated Scandinavian Redwood Pine furniture board with a density of 470 ± 10 kg/m^3 and a moisture content of 8.7 ± 0.2%. The use of a combustible floor was intended to represent other flammable objects within a compartment. The walls were formed from 25 mm thick Rockwool Beamclad which was attached to the sides of the ceiling, forming a tight seal.

For long or large fires, a 15 mm thick steel plate was placed beneath the fuel pan to act as a heat sink, so that a steady state pool fire could be maintained (this was preferred over a water bath which would interfere with the MLR measurements).

It should be noted that no downstand was present at the front of the compartment. This prevented the formation of a smoke layer within the compartment.

2.1 Instrumentation

The instrumentation comprised:

- Two independent mass balances (of readability 0.1 g) with one supporting the ceiling and walls, and the other supporting the floor and pool fire to allow quantification of the MLR of the pool fire and the time at which ignition of the ceiling and floor occurred.
- Thermocouples (Inconel sheathed, 1 mm diameter, K type) along the centreline of the compartment in the gas phase (20 mm beneath the ceiling) to allow an estimate of gas temperature above the plume and at 150 mm intervals between the pan and compartment opening. It was assumed that the impact of radiation on the gas temperature measurements were negligible.
- For selected experiments, water cooled gardon gauges were used to measure the incidient heat flux. One located in the ceiling directly above the initiating pool fire and two located in the floor at 150 mm and 300 mm from the centre of the pan.
- A video camera to allow the time of key events to be identified retrospectively.

2.2 Data Processing

The quasi-steady state HRR of the initiating pool fire preceding ignition of the ceiling was estimated using the change in mass recorded by the mass balance supporting the floor and the fuel pan. This was calculated by averaging the mass loss during the period $t_{ig,c}/2$ to $t_{ig,c}$, where $t_{ig,c}$ is the time to ignition of the ceiling. For experiments where the ceiling did not ignite, the MLR was averaged over half of the time between pan ignition and burnout, centred on the peak gas phase temperature. The HRR was calculated using an assumed combustion efficiency of 0.71 [22], and heat of combustion of 43.1 MJ/kg [23]. It was assumed that the change in mass of the bottom scale (Figure 1) prior to ignition of the floor could be attributed to the mass loss of the fuel.

The time of the ignition of the ceiling and floor were determined from the MLR recorded by the respective mass balance. The MLR data were smoothed using a 3rd degree Savitzky-Golay filter with a span of 41 data points (equivalent to approx. 40 s). The time of ignition was said to occur when the smoothed MLR began to notably rise above the noise in the MLR. This was found to align with the observed ignition time from experiments and was found to be more definitive in cases where the point of ignition was obscured by the impinging flame.

The gas phase temperature and heat flux prior to ignition were calculated by averaging their values over the minute preceding ceiling ignition. For experiments where the ceiling did not ignite, the gas phase temperature and heat flux were calculated by averaging their values over a minute centred on the peak gas phase temperature.

3. Results

Twenty-eight experiments were undertaken where a steady state pool fire was achieved. It was observed that the experiments fell into one of three categories. In eight

experiments, no ignition of the ceiling occurred (NI). In 16 experiments, ignition of the ceiling occurred, and this was followed by continuous flame spread across the ceiling (FS). In four experiments, ignition of the ceiling occurred, but was not followed by continuous flame spread, these cases are categorised as complex flame spread (CFS).

In the 16 FS experiments it was observed that flame spread occurred radially across the ceiling from the point of ignition to the compartment boundaries. This was followed by the ignition of the floor around the initiating pool fire, and subsequent flame spread across the floor from the rear of the compartment to the front, resulting in the involvement of all combustible surfaces within the compartment. This progression is shown in Figure 2.

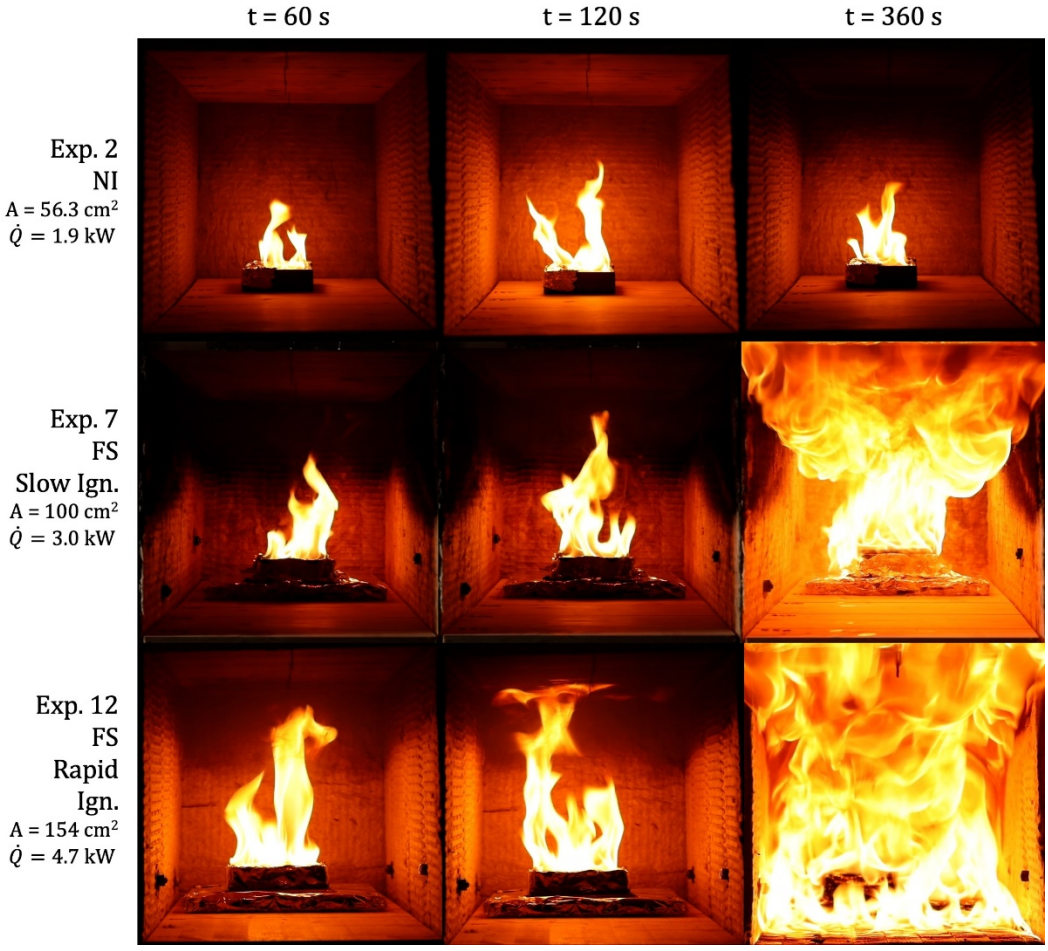

Figure 2 Images of three different experiments after 60 s, 120 s, and 360 s; thermocouple data for the same experiments are presented in Figure 3.

Figure 3 shows the temperature measurements at ceiling level directly above the initiating pool fire for all NI and FS experiments. Three experiments with identical compartment geometry but different initial HRR have been highlighted to illustrate three different behaviours: rapid ignition, slow ignition, and no ignition of the ceiling. The time at which ignition of the ceiling and floor occurred are marked on the highlighted data.

The data show that after ignition of the pool fire, the temperature of the gas increased until it achieved a quasi-steady state condition. The ceiling then ignited, leading to a further temperature increase. This was followed by the ignition of the floor. It was observed that the time between the ignition of the ceiling and the floor was greater for larger fires (this is further discussed in the analysis and discussion). This can be seen in the two experiments highlighted in Figure 3. For the experiments where ceiling ignition did not occur, the temperature of the gas remained steady until burnout occurred.

The thermocouple data showed that the temperature of the gas beneath the ceiling decreased with distance from the pool fire. This is shown illustratively in Figure 4.

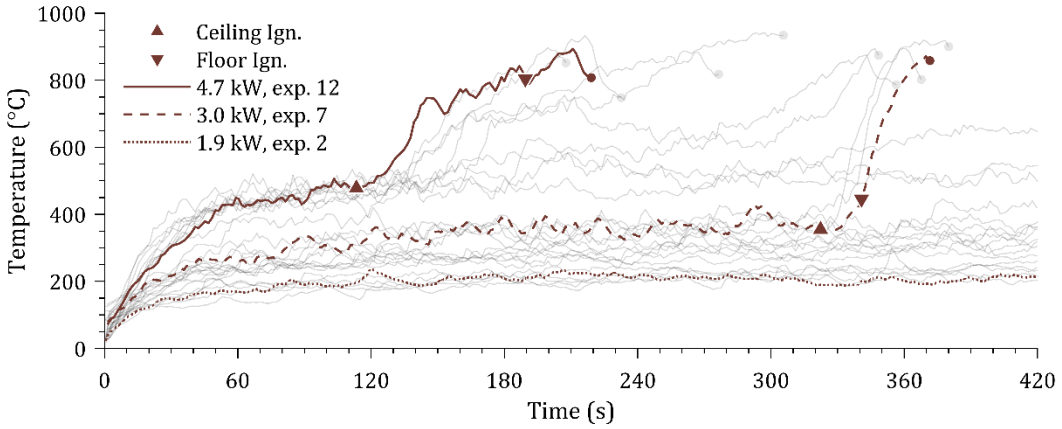

Figure 3 Temperature beneath the ceiling directly above the initiating fire with three experiments highlighted (Exp. 12, 7 & 2, as presented in Figure 2). For clarity, the data have been curtailed 30 s after the ignition of the floor – represented by a circle.

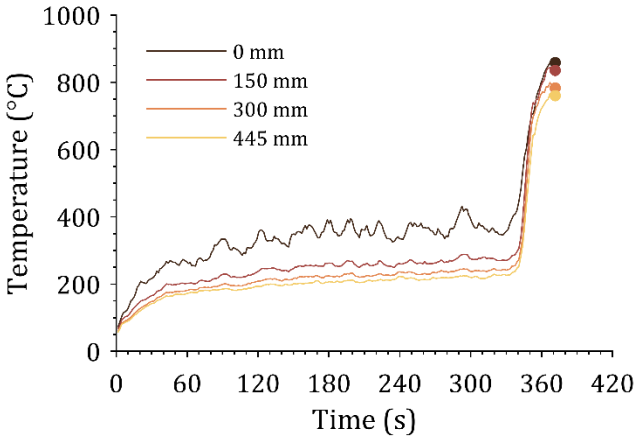

Figure 4 Example temperature evolution of the gas beneath the ceiling at different distances from the point of flame impingement(Exp. 7). For clarity, the data have been curtailed 30 s after the ignition of the floor – represented by a circle.

In four experiments, the flame spread across the ceiling following ignition was categorised as “complex”. In these experiments, the flames did not spread continuously across the entire ceiling following ignition. Instead, flaming was localized around the point of ignition for a period until the flaming ceased. After further exposure to the initiating fire, the ceiling of three of these experiments ignited again. It was observed that, following second ignition of the ceiling, flames spread across the entire ceiling and the floor ignited, leading to full involvement of all combustible surfaces. An example is shown in Figure 5 – where the double ignition of the ceiling can be seen in both the temperature data and the mass loss data. The “complex” behaviours were observed during the experiments with the widest compartment (600 mm).

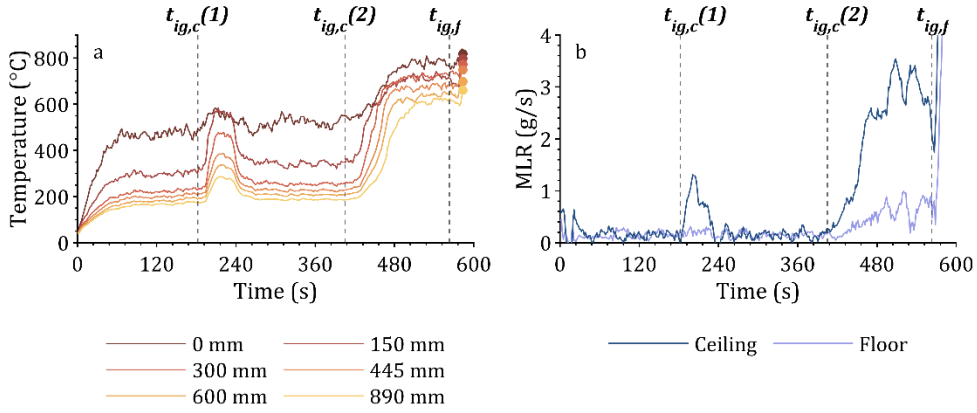

Figure 5 Example of a) temperature and b) MLR of a CFS exp. (Exp. 25)

The compartment geometry, key parameters and results from each experiment have been summarised in Table 1. The variable z is the distance between the seat of the pool fire and the ceiling and accounts for: the thickness of the steel plate (where present), the thickness of the pan and half of the level of the fuel.

Table 1 Experimental matrix and key results

#		A cm^2	h mm	d mm	w mm	z mm	$\dot{m}$ g/s	$\dot{Q}$ kW	T °C	$t_{ig,c}$ s	$t_{ig,f}$ s
1	NI	50.4	300	600	300	268	0.070	2.1	300	-	-
2	NI	56.3	300	600	300	268	0.061	1.9	245	-	-
3*	NI	56.3	300	600	300	253	0.040	1.2	224	-	-
4	FS	69.6	300	600	300	268	0.102	3.1	360	488	506
5	FS	100	300	600	300	268	0.111	3.4	375	325	336
6	FS	100	300	600	300	268	0.094	2.9	347	414	423
7	FS	100	300	600	300	253	0.097	3.0	372	321	340
8*	FS	100	300	600	300	253	0.088	2.7	358	322	349
9*	FS	117	300	600	300	243	0.128	3.9	466	128	305
10	FS	122	300	600	300	243	0.154	4.7	469	156	246
11	FS	122	300	600	300	243	0.170	5.2	483	141	326
12	FS	154	300	600	300	253	0.153	4.7	454	113	189

13	FS	154	300	600	300	253	0.160	4.9	476	122	202
14*	FS	154	300	600	300	253	0.100	3.1	455	131	177
15	NI	100	345	600	300	298	0.110	3.4	328	-	-
16	NI	100	345	600	300	298	0.097	3.0	307	-	-
17	FS	117	345	600	300	288	0.148	4.5	384	535	553
18	FS	119	345	600	300	288	0.104	3.2	368	545	552
19	NI	100	390	600	300	343	0.105	3.2	280	-	-
20	NI	100	390	600	300	343	0.102	3.1	273	-	-
21	FS	117	390	600	300	333	0.161	4.9	355	681	703
22	FS	117	390	600	300	333	0.151	4.6	362	803	806
23	NI	56.3	300	1200	600	253	0.050	1.5	228	-	-
24	FS	100	300	1200	600	253	0.116	3.6	397	465	540
25	CFS	117	300	1200	600	243	0.160	4.9	477	172	553
26	CFS	117	300	1200	600	243	0.165	5.0	448	129	-
27	CFS	117	300	1200	600	243	0.151	4.6	503	158	498
28	CFS	154	300	1200	600	253	0.130	4.0	476	174	317

*Experiments conducted with heat flux gauges

During four experiments (each with the base configuration) the incident heat flux to the ceiling and the floor was measured (marked in Table 1). An example of the evolution of the heat flux with time is presented in Figure 6. This plot shows that the heat flux at the ceiling above the pool fire reaches a quasi-steady state (albeit with substantial variability) prior to the ignition of the ceiling and the heat flux to the ceiling and floor increase after ignition of the ceiling. This graph also shows that the ignition of the ceiling and floor occurred at similar heat fluxes (20.9 kW/m^2 and 30.7 kW/m^2 respectively).

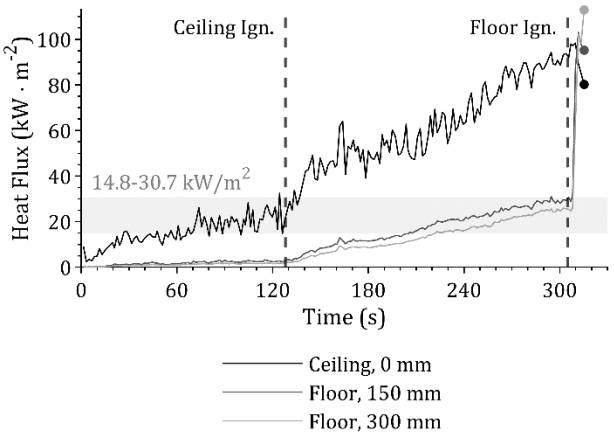

Figure 6 Typical heat fluxes recorded with ignition of the ceiling and floor indicated (Exp. 9). The range of heat fluxes recorded at ignition of the ceiling and floor are highlighted.

The heat fluxes recorded prior to the ignition of the ceiling and floor are presented in Table 2. This data show that (unsurprisingly) larger pool fire HRR leads to higher heat fluxes above the fire. A notable observation from the data is that for Exp. 9 (2.8 kW), the incident heat flux to the floor was significantly greater than during the other experiments – these are highlighted in bold in Table 2. The recorded video footage indicates that the floor in this experiment ignited through autoignition (as opposed to piloted ignition in the case of the other experiments).

Table 2 Recorded heat flux (HF) prior to ignition of the ceiling and floor.

#		$\dot{Q}$ kW	$t_{ig,c}$ s	$t_{ig,f}$ s	Δt_{ig} s	Incident Heat flux Ceiling $t = t_{ig,c}$ x = 0 mm kW/m^2	Floor $t = t_{ig,c}$ / $t = t_{ig,f}$ x = 150 mm kW/m^2	x = 300 mm kW/m^2
3	NI	0.91	-	-	-	7.83*	1.04*	0.66*
8	FS	2.1	322	349	27	15.2	2.2 / 17.8	1.44 / 13.2
9	FS	2.8	128	305	177	20.9	2.6 / **30.7**	1.69 / **25.4**
14	FS	2.5	131	177	46	20.7	2.7 / 14.8	1.96 / 11.6

*Steady state HF for comparison as no ignition occurred in this case.

4. Analysis

The initiating fire HRR and compartment geometry were systematically varied, and the temperature beneath the ceiling where the initiating fire impinged was recorded. This allowed the results to be compared with the existing fit against Eq. 1 for the variation of temperature rise with height from the base of the fire and convective portion of the heat release rate of the fire $\dot{Q}_c$ (assumed to be 70% of the values reported in Table 1 ([5] pg. 136)).

These data are presented in Figure 7 alongside the original data. Horizontal error bars indicate the combined standard error of the height above the pool fire (that will vary as the fuel is consumed) and standard error of the noise in the HRR. This comparison shows that the results align with the previous work. The markers are shaded to indicate whether the ceiling ignited (red) or not (blue). The results show a clear divide between the experiments where the ceiling ignited and those where it did not. From these results, the critical ignition temperature lies between 328°C and 347°C. This is within the range of ignition temperatures of timber reported in literature [24].

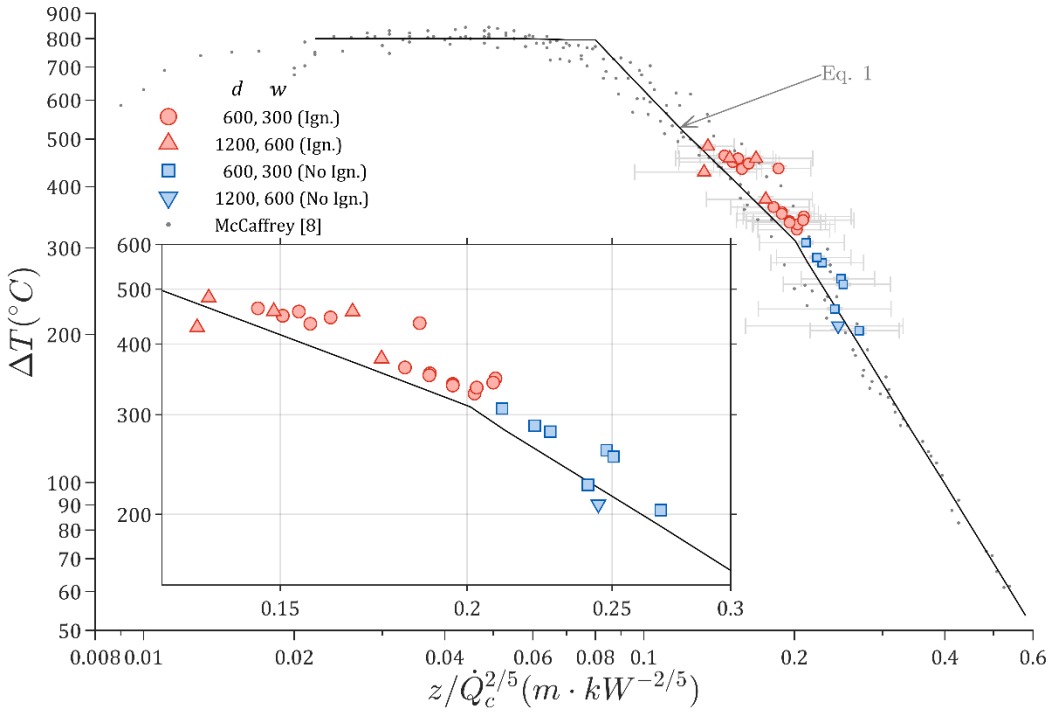

Figure 7 Comparison between the data in ref. 6, and the data from this study with gathered data. The depth and width of the compartments are given in millimetres.

Following ignition of the ceiling, the flame spread across the ceiling and ignition of the floor occurred. It was observed that the elapsed time between the ignition of the ceiling and floor was greater for experiments where the time to ignition of the ceiling was short. The ignition times of the ceiling and floor are presented in Figure 8 and the variation of time difference with ignition time is presented in Figure 9. These data were sorted by ceiling ignition time for presentation in this format. These figures show the importance of the duration of preheating prior to ignition. The video data showed that for the majority of the experiments, ignition of the floor was piloted by the fuel burning in the pan. However, for the two experiments where there was a relatively long elapsed time between ignition of the ceiling and floor, the floor was observed to ignite through autoignition (i.e. the pyrolyzate was not observably ignited due to contact with the pool fire). The heat fluxes recorded in the floor, 150 mm from the centre of the pool fire, at ignition are marked on Figure 9. This shows that the heat flux was significantly higher for the two experiments with the larger time difference between ignitions. This corroborates the notion that the increased elapsed time between ignition of the ceiling and floor was due to the absence of piloted ignition in these cases.

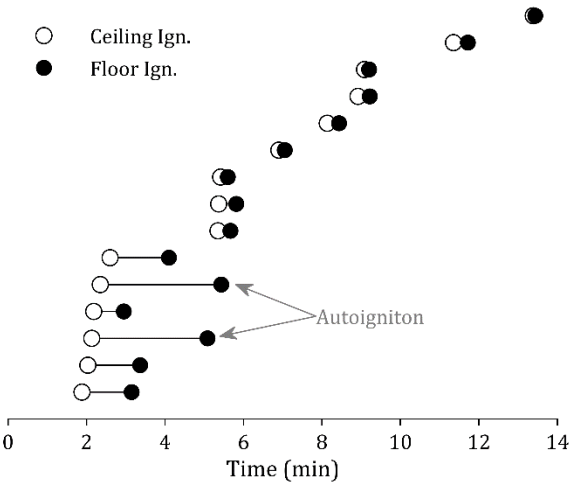

Figure 8 Time to ignition of the ceiling and floor for narrower compartments

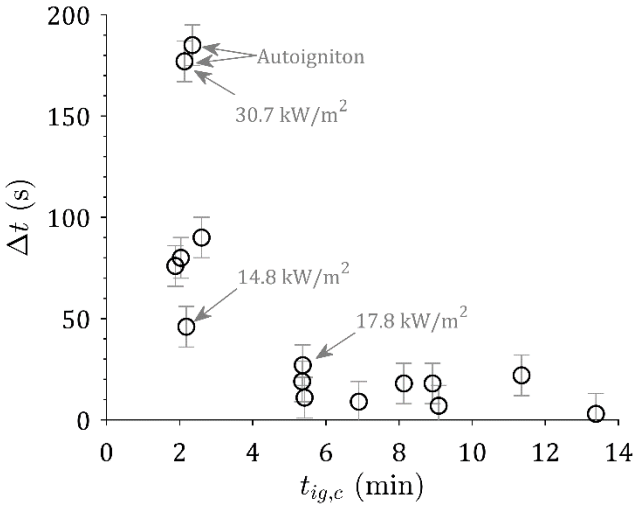

Figure 9 Time between ignition of the ceiling and floor against the time to ignition of the ceiling for narrower compartments. For experiments where the heat flux was measured, the heat fluxes recorded in the floor, 150 mm from the centre of the pool fire, at ignition are presented.

The preheating of the ceiling is dependent on the condition of the ceiling jet beneath the ceiling. The temperature of a radially expanding (i.e. unconstrained) ceiling jet is predicted by Eq. 2. During this experimental programme the ceiling jet was constrained by the side walls of the compartment – and was not, therefore, free to expand radially in all directions. Nevertheless, the scaling parameters in Eq. 2 (i.e. initiating fire HRR, height of rise, and distance from source) remain relevant to the conditions within the ceiling jet. The temperature, prior to ceiling ignition, 300 mm from the point of impingement was plotted using these scaling parameters (figure 10). The temperature measurements are remote from the impinging flames and are referred to as the “far field” temperatures. This plot shows that Eq. 2 remains useful comparing different

temperatures as a function of initial fire HRRs and heights of rise, but that the absolute value of the temperature (and therefore the constant of proportionality for the scaling parameter) is significantly influenced by the presence of the compartment boundaries. The narrower compartment gave the highest temperatures, while the wider compartment gave lower temperatures. This is due to the reduced entrainment into the ceiling jet due to the reduced area over which entrainment can occur compared to a radially expanding ceiling jet. Where the constraint is greater (i.e. the smaller compartment), then the temperatures are higher. Alpert's correlation (for an unconstrained expansion of the ceiling jet) is plotted to show the lower bound.

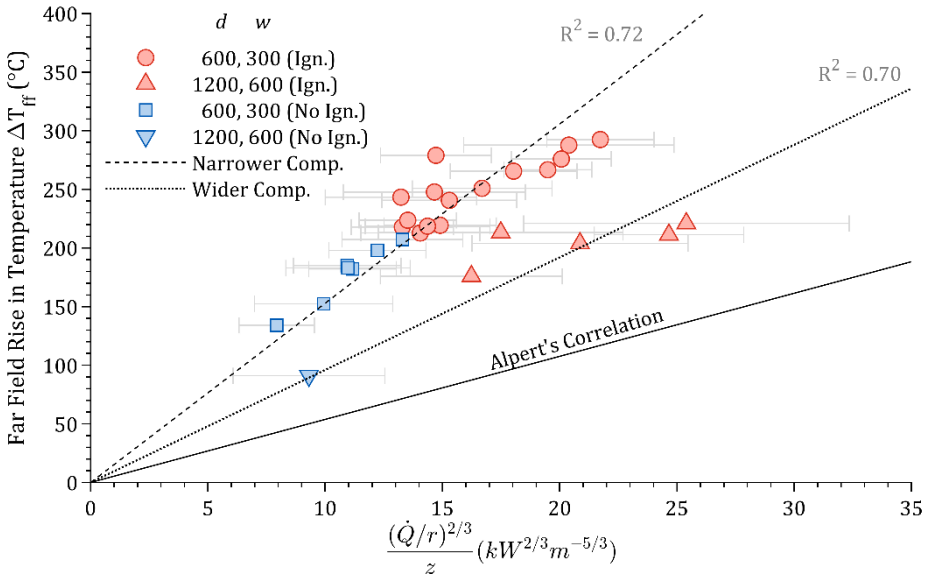

Figure 10 Scaling of far field temperature using Alpert's scaling parameters. The depth and width of the compartments are given in millimetres.

5. Discussion

The temperature increases in the gas phase beneath the ceiling and above a pool fire in a reduced scale compartment show strong agreement with Eq. 1 and its supporting data. This echoes previous findings in the context of plume impingement [14] – even though the original data were developed for an unconfined plume. The results indicate that ignition of the ceiling can be expected where temperatures in the gas phase are in the region of 350 °C. Conversely, ignition was not observed where temperatures were below approximately 330 °C. These values are consistent with ignition temperature thresholds from the literature. This result demonstrates the potential of existing methods to remain useful during application to buildings with exposed timber ceilings. The results suggest that if the gas phase temperature does not exceed 330 ºC, the ignition of the ceiling – and subsequent rapid fire spread through the compartment – may be prevented.

However, it should be noted that the volume of fuel used in the pool fires was intended to burn for up to 20 minutes (after which time the ceiling was no longer considered thermally thick). If the duration of the pool fire was extended and thickness of timber

increased, then it is possible that some of the experiments where no ignition was observed would have ignited. The potential for substantially delayed ignition of timber has been demonstrated in a set of experiments conducted by Spearpoint and Quintiere, where one sample ignited after 93 minutes of exposure to a constant heat flux of 12 kW/m^2 [24].

The presence of compartment boundaries significantly impacts the temperature of the ceiling jet by limiting entrainment, resulting in greater gas temperatures. This was highlighted in the compartments with a greater width where the ceiling jet temperatures were lower (all other factors being equal). In some cases, it was possible for ignition *not* to be followed by immediate fire spread – due to a low level of pre-heating. This illustrates the importance of the entrainment of cool air in the fire spread rate across combustible ceilings.

Growth to flashover rapidly follows flame spread on the ceiling. However, this aspect of the experiment was not well controlled as in some cases pyrolysate from the floor was ignited by a pilot (the pool fire), and in some cases pyrolysate from the floor auto-ignited. This indicates that the final event that leads to full involvement of the compartment is stochastic in nature.

6. Conclusion

Evaluation of the hazard posed by timber ceilings in compartments requires knowledge of plume behaviour, conditions for the ignition of timber, flame spread on ceilings, and flashover. Reduced scale experiments have demonstrated that existing knowledge of plume and timber behaviour can be used to determine when ignition of exposed timber ceilings may occur – when subject to heating from a “small” free field pool fire within a compartment. The results show that ceiling ignition, flame spread, and flashover are governed by different processes. It was found that:

- There was alignment between measured temperatures within the plume above the pool fire and the McCaffrey’s plume correlation [6]. This alignment was found to be a useful method for predicting if ceiling ignition would occur.
- The preheating of the ceiling and conditions in the smoke layer (or ceiling jet) strongly influenced whether flames spread across the ceiling once ignited.
- Spread of the fire on the ceiling resulted in a significant increase in heat flux to the floor, which ultimately led to its ignition, and therefore flashover.
- Once flames had spread across the ceiling, the time delay to ignition of the floor was heavily influenced by stochastic behaviours (i.e. whether the pyrolysis gases were piloted by the pool fire or ignited only due to auto-ignition).

The experimental programme allowed the stages of fire development to be systematically examined. These experiments show the utility of existing knowledge in evaluating this hazard, and also the usefulness of relatively small-scale investigations for elucidating the underpinning phenomena that may be observed in larger experiments.

However, the scale of these experiments also introduces a limitation. The magnitude of the initiating fire remained constant once established; a fire in a real compartment would be expected to grow, whereas the fire in this experimental programme was constrained to the size of the pan. Similarly, while the scaling analyses are (obviously) intended to be scale independent, these findings have not been corroborated at large scale, and in a design context, should therefore be used with caution.

7. References

[1] D. Barber, D. Blount, J. Hand, M. Roelofs, L. Wingo, J. Woodson, F. Yang, Design Guide 37: Hybrid Steel Frames with Wood Floors, (2022).

[2] B. Sundström, P. Van Hees, P. Thureson, Results and analysis from fire tests of building products in ISO 9705, the Room/Corner Test. The SBI Research programme., 1998.

[3] Forest Products Laboratory, Wood handbook: Wood as an engineering material. General Technical Report FPL-GTR-282., U.S. Department of Agriculture, Forest Service, Forest Products Laboratory, Madison, WI, 2021.

[4] A.I. Bartlett, R.M. Hadden, L.A. Bisby, A Review of Factors Affecting the Burning Behaviour of Wood for Application to Tall Timber Construction, Fire Technology 55 (2019) 1–49. https://doi.org/10.1007/s10694-018-0787-y.

[5] D. Drysdale, An Introduction to Fire Dynamics, Third, Wiley, Chichester, 2011.

[6] J. Quintiere, Fundamentals of Fire Phenomena, Wiley, West Sussex, England, 2006.

[7] B.R. Morton, G. Taylor, J.S. Turner, Turbulent Gravitational Convection from Maintained and Instantaneous Sources, Proceedings of the Royal Society of London. Series A, Mathematical and Physical Sciences 234 (1956) 1–23.

[8] B. McCaffrey, Purely Buoyant Diffusion Flames: Some Experimental Results, Centre for Fire Research National Bureau of Standards, 1979.

[9] National Fire Protection Association, NFPA 92 Standard for Smoke Control Systems, (2024).

[10] CIBSE, Guide E: Fire safety engineering, (2019).

[11] T.J. Shields, G.W. Silcock, J.J. Murray, The effects of geometry and ignition mode on ignition times obtained using a cone calorimeter and ISO ignitability apparatus, Fire and Materials 17 (1993) 25–32. https://doi.org/10.1002/fam.810170105.

[12] R.L. ALPERT, Turbulent Ceiling-Jet Induced by Large-Scale Fires, Combustion Science and Technology 11 (1975) 197–213. https://doi.org/10.1080/00102207508946699.

[13] H.Z. You, G.M. Faeth, Ceiling heat transfer during fire plume and fire impingement, Fire and Materials 3 (1979) 140–147. https://doi.org/10.1002/fam.810030305.

[14] M.A. Kokkala, Experimental study of heat transfer to ceiling from an impinging diffusion flame, in: Fire Safety Science - Proceedings of the Third International Symposium, 1991: pp. 261–270.

[15] M.A. Kokkala, Heat transfer to and ignition of ceiling by an impinging diffusion flame, VTT, 1989.

[16] S. Nothard, D. Lange, J.P. Hidalgo, V. Gupta, M.S. McLaggan, F. Wiesner, J.L. Torero, Factors influencing the fire dynamics in open-plan compartments with an

exposed timber ceiling, Fire Safety Journal 129 (2022) 103564. https://doi.org/10.1016/j.firesaf.2022.103564.
[17] P. Kotsovinos, E. Rackauskaite, E. Christensen, A. Glew, E. O'Loughlin, H. Mitchell, R. Amin, F. Robert, M. Heidari, D. Barber, G. Rein, J. Schulz, Fire dynamics inside a large and open-plan compartment with exposed timber ceiling and columns: CodeRed #01, Fire and Materials n/a (2022). https://doi.org/10.1002/fam.3049.
[18] D.D. Drysdale, A.J.R. Macmillan, Flame spread on inclined surfaces, Fire Safety Journal 18 (1992) 245–254. https://doi.org/10.1016/0379-7112(92)90018-8.
[19] M.J. Gollner, X. Huang, J. Cobian, A.S. Rangwala, F.A. Williams, Experimental study of upward flame spread of an inclined fuel surface, Proceedings of the Combustion Institute 34 (2013) 2531–2538. https://doi.org/10.1016/j.proci.2012.06.063.
[20] P.L. Hinkley, H.G. Wraight, The contribution of flames under ceilings to fire spread in compartments Part II. Combustible ceiling linings. Fire Research Note 743, FRS, 1969.
[21] X. Chen, X. Yu, Y. Lin, G. Li, J. Wang, R. Zong, Experimental Study on Flame Extension and Pattern Analysis of Jet Fire Impinging Wood Plates, Fire Technology (2022). https://doi.org/10.1007/s10694-022-01338-8.
[22] A. Tewarson, Experimental Evaluation of Flammability Parameters of Polymeric Materials, in: M. Lewin, S.M. Atlas, E.M. Pearce (Eds.), Flame - Retardant Polymeric Materials: Volume 3, Springer New York, Boston, MA, 1982: pp. 97–153. https://doi.org/10.1007/978-1-4757-0112-8_3.
[23] M.J. Hurley, ed., SFPE Handbook of Fire Protection Engineering, 5th ed., Springer, 2016.
[24] M.J. Spearpoint, J.G. Quintiere, Predicting the piloted ignition of wood in the cone calorimeter using an integral model — effect of species, grain orientation and heat flux, Fire Safety Journal 36 (2001) 391–415. https://doi.org/10.1016/S0379-7112(00)00055-2.